PHILOSOPHICAL TRANSACTIONS OF THE ROYAL SOCIETY A MATHEMATICAL, PHYSICAL & ENGINEERING SCIENCES

Modelling Arctic Climate Change [and Discussion]

H. Cattle, J. Crossley and D. J. Drewry

Phil. Trans. R. Soc. Lond. A 1995 **352**, 201-213
doi: 10.1098/rsta.1995.0064

Modelling Arctic climate change

By H. Cattle and J. Crossley

Hadley Centre for Climate Prediction and Research, Meteorological Office, Bracknell, Berkshire, RG12 2SY

Climate prediction requires the use of coupled models of the atmosphere–deep ocean–sea ice and land surface. This paper outlines the formulation of processes relevant to the simulation and prediction of climate change in the Arctic of one such model, that of the Hadley Centre for Climate Prediction and Research at the Meteorological Office. Comparison of the simulation of a number of features of the Arctic climate is made against observations and predictions of future climate change resulting from increased concentrations of greenhouse gases from recent runs of the model are discussed.

1. Introduction

Prediction of future climate change due to increased concentrations of greenhouse gases resulting from the burning of fossil fuels and other human activities requires the use of coupled models of the climate system. Such models consist of a number of component physical models (of the atmosphere, land surface, oceans and sea ice) which are interactively 'coupled' by exchange of information across the interfaces between them. Thus, for example, the fluxes (of heat, freshwater and momentum) which drive the ocean are calculated within the atmospheric model and passed across to the ocean model. The ocean model in turn calculates new values of sea surface temperature which are passed back to the atmospheric model in the next phase of its integration. This, then, provides an interactive coupling between the atmosphere and ocean model components.

The aim in the construction of such models is to represent the key processes and feedbacks important for climate prediction and for studies of climate variability. Previously they have shown the Arctic to be a region of high climate sensitivity to increased concentrations of greenhouse gases (see Houghton *et al.* 1990, 1992). In this paper we describe some aspects of the Arctic simulation of one such model, that of the Hadley Centre for Climate Prediction and Research at the Meteorological Office, and outline its current projections of future climate change over the region. However, it must be borne in mind that confidence in the ability of climate models to represent regional climate change is as yet rather low (Houghton *et al.* 1990, 1992). Nevertheless, the sensitivity of the Arctic to increased concentrations of greenhouse gases is a consistent feature of global climate model simulations. This is seen both in sensitivity studies to instantaneous doubling of greenhouse gases using atmospheric models coupled to simple 'slab' ocean models (see Manabe & Stouffer 1980; Washington & Meehl 1986; Wilson & Mitchell 1987; see also Houghton *et al.* 1990, 1992) and in model runs to study the 'transient' response to gradually increasing concentrations

Phil. Trans. R. Soc. Lond. A (1995) **352**, 201–213
Printed in Great Britain

of greenhouse gases (e.g. Manabe *et al.* 1991, 1992; Cubash *et al.* 1992; Murphy 1995; Murphy & Mitchell 1995). Such runs require atmospheric models to be coupled to dynamical models of the ocean, allowing ocean processes to be represented throughout its entire depth. For a recent review of the Arctic sensitivity of models to increased greenhouse gases, see Rowntree (1993).

2. Model description

The model used in the experiments described here is a version of the Meteorological Office unified model for numerical weather prediction and climate studies (Cullen 1993). In climate mode, the atmospheric model is run coupled to ocean, sea ice and land surface models on a $2.5° \times 3.75°$ latitude–longitude grid. The atmospheric model has 19 levels in the vertical and the ocean model 20. The atmospheric model incorporates the interactive radiation scheme of Ingram (1990), the prognostic cloud scheme of Smith (1990) (which includes explicit representation of cloud liquid water), a penetrative convection parametrization based on Gregory & Rowntree (1990), but with the addition of a representation of the effects of convective downdraughts and a gravity wave drag scheme based on the work of Palmer *et al.* (1986). The ocean model is based on that of Cox (1984) with the addition of an upper-ocean mixed-layer scheme based on Kraus & Turner (1967), the shear induced mixing parametrization of Pacanowski & Philander (1981) and the isopycnal mixing scheme of Redi (1982). The land surface scheme is based on that of Warrilow *et al.* (1986).

A key feature of high-latitude climate is its snow and ice cover. In the model, snow falling on the land surface accumulates there when the surface temperature is below 0 °C. Snow depth is allowed to change interactively over the model's land surface through the processes of accumulation, sublimation/deposition and melting. Over land, a snow albedo formulation is used which depends on snow depth, the snow-free albedo of the surface, a deep snow albedo for temperature and vegetation type and, near the melting point, on temperature. Surface temperature, T_*, changes as a function of time, t, according to the prognostic equation:

$$C_* \partial T / \partial t = R_N + H + LE + G, \tag{1}$$

where C_* is the effective surface thermal capacity, R_N is the net solar plus longwave surface radiative flux, H is the surface sensible heat flux, E is the surface evaporative flux, L the latent heat of vaporization (or, if the suface is snow covered, of sublimation) and G is the soil heat flux. If snow is present, then snow melt is allowed to occur when the surface temperature is predicted by (1) to rise above 0 °C. In that case, the surface temperature is reset to the melting point and the excess energy is used to melt snow.

Snow accumulation and melting on the surface of sea ice is also represented in the model. Sea ice forms within the ocean model when the surface temperature of the surface layer over a given model timestep falls below the freezing point of sea water (−1.8 °C) or as a result of advection out from the ice edge. In that case, the layer temperature is reset to the freezing point and a sufficient covering of sea ice (of initial mean thickness 0.5 m) is allowed to form to ensure that conservation of heat is satisfied. The model thus allows fractional sea-ice coverage. The formulation of fractional ice cover is based on that of Hibler (1979), which assumes the ice covered area to have a uniform ice thickness distribution of mean thickness h_{I}. The atmospheric

model calculates surface radiative and turbulent heat fluxes separately for ice and open water (leads) over grid squares which include sea ice.

A simple ice thickness advection scheme is used in the model following Bryan *et al.* (1975), in which the rate of change of mean ice thickness over a grid square changes according to:

$$\partial h_{\mathrm{I}}/\partial t = \nabla \cdot (\delta_h \boldsymbol{v} h_{\mathrm{I}}) + A_H \nabla^2 h_{\mathrm{I}} + \text{thermodynamic changes}, \tag{2}$$

where $\boldsymbol{v}$ is the ocean current vector in the surface layer of the model ocean; A_H is the ocean thermal diffusivity and $\delta_h = 1$ for $h < 4$ m, 0 for $h > 4$ m. Though simple, introduction of this formulation produces a marked improvement in the model's representation of the seasonal variation of sea ice in the southern hemisphere in particular (cf. Cattle *et al.* 1993), and removes the need for flux correction (see below) of the sea ice itself, though these are still applied to ocean beneath the ice.

The sea ice thermodynamics formulation used in the model follows the zero-layer model of Semtner (1976) in which the ice–snow layer is treated as a single slab. The surface temperature of the ice changes according to the same heat balance equation as (1), in which G now becomes the heat conduction through the ice, H_{I}, given by the equation:

$$H_{\mathrm{I}} = k_{\mathrm{S}}(T_{\mathrm{S}} - T_{\mathrm{F}})/[h_{\mathrm{S}} + (h_{\mathrm{I}} k_{\mathrm{S}}/k_{\mathrm{I}})], \tag{3}$$

where k_{S} and k_{I} are the thermal diffusivities of snow and ice; h_{S} and h_{I} the snow and ice layer thicknesses and T_{S} and T_{F} the ice/snow surface and ice bottom temperatures respectively. T_{F} is assumed to be at the freezing point of seawater (taken as $-1.8\,^{\circ}$C), as is the surface temperature of leads.

For surface temperatures below $-10\,^{\circ}$C, the snow/ice surface albedo is taken to have a constant value of 0.8. Above this temperature, ice albedo decreases linearly to a value of 0.5 at the melting point ($0\,^{\circ}$C) to allow for the lowering of albedo caused by the presence of melt ponds on the ice surface. The albedo of leads is assumed to be a constant 0.06.

Any net heat flux entering (or leaving) the leads is partitioned between ice melt (or ice formation) and warming (or cooling) of the upper layer of the ocean. The partitioning between ice melt/formation and ocean warming/cooling is chosen to be directly proportional to the ice area. Ocean temperatures less than $-1.8\,^{\circ}$C also result in ice formation. Ocean surface layer temperatures higher than $-1.8\,^{\circ}$C result in a bottom heat flux from the ocean to the ice given by:

$$H_{\circ} = \rho c k (T_1 - T_{\mathrm{F}})/0.5\Delta z_1,$$

where ρ is the density and c the specific heat capacity of seawater, k is an 'eddy diffusivity', taken as 2.5×10^{-3} m^2 s^{-1} and T_1 is the temperature of the uppermost layer of the model ocean, of depth Δz_1.

At the ice surface, snow melt (or, if no snow is present, ice melt) occurs in the model under the same conditions as for snow on the land surface. Any meltwater formed is passed to, and freshens, the surface layer of the ocean model. Alternatively, brine release associated with ice formation leads to reduced freshening. More generally over the model oceans, salinity can change depending on the sign of the precipitation minus evaporation difference. Surface freshening (important for the Arctic salinity balance) can also occur as a result of runoff from the model's land surface which is formulated following the scheme described by Taylor & Bunton (1993).

Because of the relatively long timescales on which they respond to change, the

PHILOSOPHICAL TRANSACTIONS OF THE ROYAL SOCIETY A MATHEMATICAL, PHYSICAL & ENGINEERING SCIENCES

major land ice sheets of Greenland and Antarctica are treated non-interactively in the model with the ice mass held fixed and specified through the model's topography field. A constant surface albedo of 0.8 is used over land ice.

3. Model performance over the Arctic

In this section, we illustrate the ability of the coupled system to represent some of the major features of Arctic climate. The fields shown here are from a run of the model with constant greenhouse gas concentrations used as a control against which to compare scenario runs with increased greenhouse gas concentrations (Hadley Centre 1995). The runs followed a long spin-up integration of the coupled system in which sea surface temperatures and salinities were relaxed back to their seasonally varying climatological observed values. Thus, for example, in specifying the net heat flux into the ocean, this quantity was modified by the addition of a term:

$$-\lambda(T_m - T_c)$$

where T_m and T_c are the model's instantaneous and the observed climatological sea surface temperatures (SSTs) respectively and λ is a relaxation coefficient (taken in the runs described here to have a value of 165 W m^{-2}K^{-1}). Towards the end of the spinup integration, these terms were averaged to form seasonally and geographically varying flux correction fields which were then applied during the control and scenario runs. Such an artifact is commonly used in the present generation of climate models (see Cubasch *et al.* 1992; Manabe *et al.* 1991; Murphy 1995) and is necessary to remove the drifts which would otherwise occur in the model climate.

Figure 1 shows the surface mean sea level pressure field over the Arctic for January and July as observed and as simulated by the model. Proper simulation of the surface pressure field is important since the associated wind field provides the primary dynamical forcing on sea ice. In winter (figure 1*a*), the observed surface pressure field is dominated over the Atlantic by the Icelandic low which extends northeastwards over the Greenland Sea into the eastern Arctic. A ridge of high pressure extending across the Arctic to the north of the Bering Strait links the winter high pressure systems over the American and Eurasian continental areas; to the south of the Bering Strait lies the Aleutian low. This pattern begins to evolve during March and April towards the summer pattern of figure 1*b* in which a weak ridge extends across the Arctic linking the high pressure systems extending northeastwards from the Pacific and Azores highs. The return to the winter pattern begins to take place in September. The model gives a good representation of the seasonal evolution of the surface pressure patterns, illustrated by figures 1*c* and *d*, which show the simulated patterns for January and July.

For January, the model shows the Icelandic trough in winter to be associated with the zone of maximum precipitation and cloud, with rather lower cloud amounts and low precipitation values lying along the high pressure ridge over the central Arctic (figure 2*c* and *d*). These features are borne out in observational fields given by Legates & Willmott (1990) (figure 2*a* and *b*) for precipitation and, for example, in the cloudiness fields shown by Orvig (1970). The seasonal evolution of modelled total cloud amount for the area north of 60° N is compared with surface-based observed values in figure 3. The model shows perhaps too much cloud overall, with a reduced seasonal cycle, though the climatology is uncertain, especially in winter. The modelled seasonal evolution of precipitation over sea ice polewards of 75° N (figure 4)

PHILOSOPHICAL TRANSACTIONS OF THE ROYAL SOCIETY A MATHEMATICAL, PHYSICAL & ENGINEERING SCIENCES

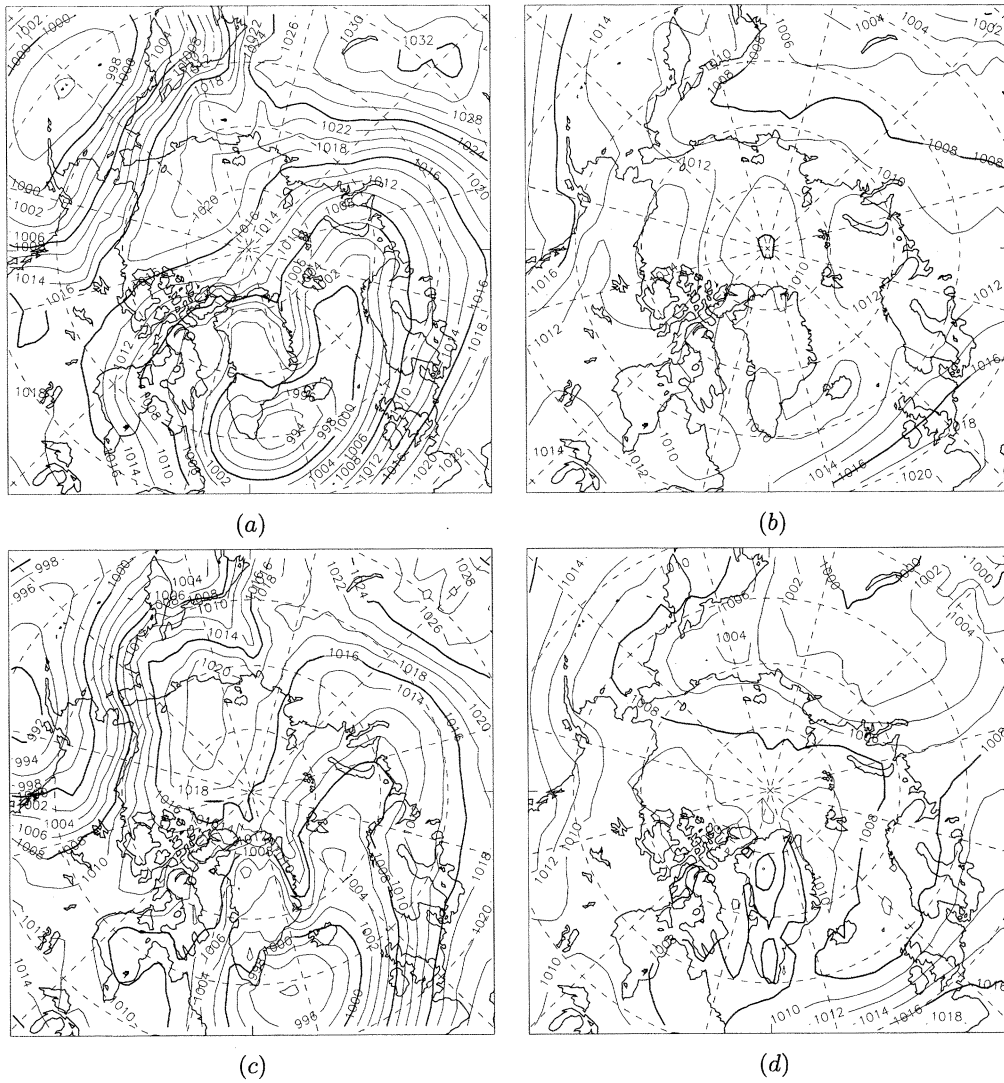

Figure 1. Mean sea level pressure over the Arctic as observed for (*a*) January and (*b*) July and modelled for (*c*) January and (*d*) July. Observed fields are derived from UK Meteorological Office operational analyses.

shows a marked seasonal variation with area averaged precipitation a minimum in spring and a maximum in autumn. Overall amounts over the year given by the model are somewhat higher overall than the typical annual mean figure of 0.5 mm day^{-1} (see the dataset of Legates & Willmott (1990)), though, again, the climatology over the central Arctic basin is uncertain.

The pattern of surface temperature shown by the model for January is shown in figure 5*a*. Observed fields (see Orvig 1970) show surface air temperatures in January to be coldest (down to −50 °C or more) over the Greenland ice cap, and the Siberian land mass, where lowest mean temperatures are below −40 °C. Over the Arctic basin itself, the coldest air is found on the northern side of the Canadian Archipelago with average temperatures down to −34 °C. A tongue of warmer air penetrates the Arctic via the northeastwards extension of the Icelandic trough and, to a lesser extent in the

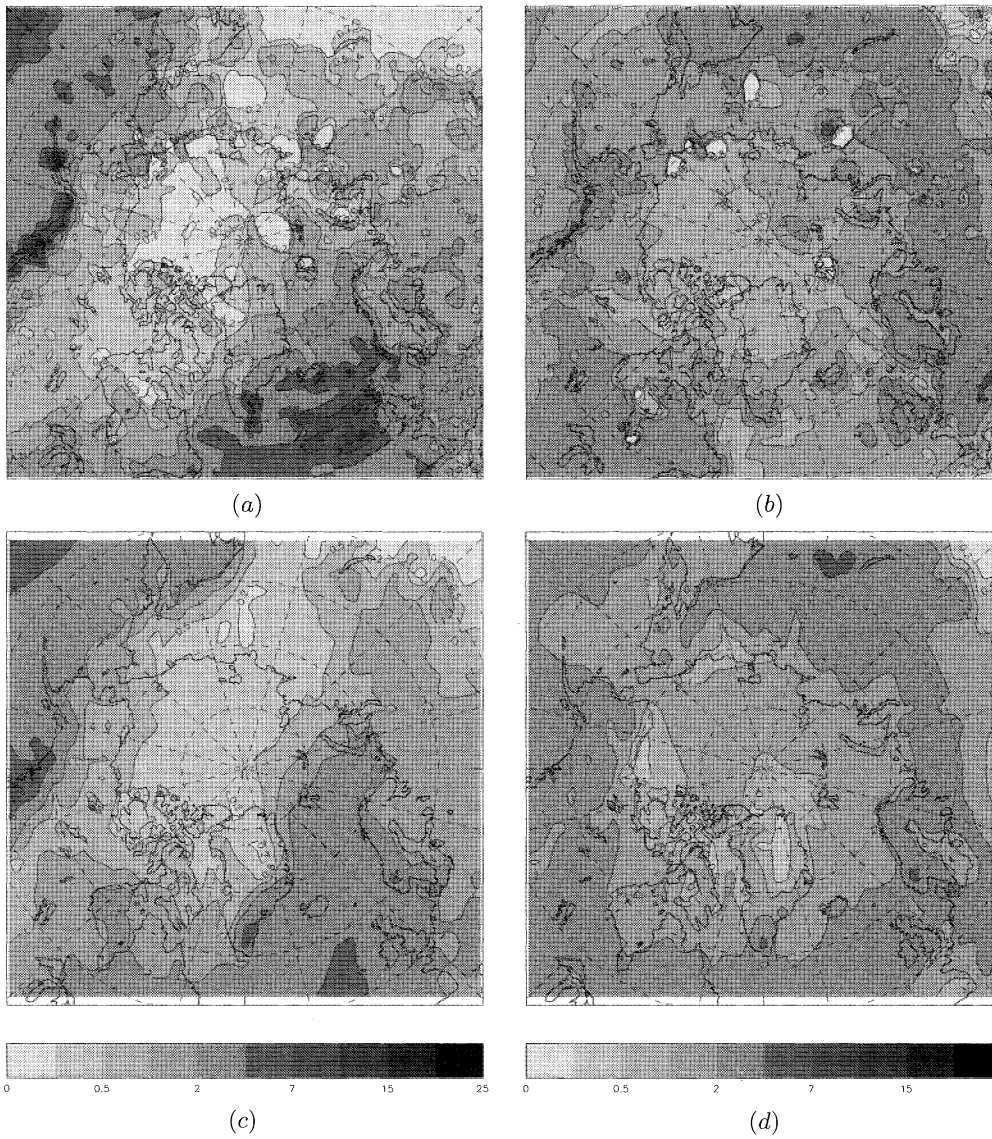

Figure 2. As figure 1, but for precipitation. Observed fields are derived from the dataset of Legates & Willmott (1990).

region of the Bering Strait. Overall, these features are well captured by the model. In summer (figure 5*b*), surface temperatures over the pack ice are constrained to lie near freezing by the melting snow and ice surface. Comparison of the seasonal evolution of ice surface temperature polewards of 75° N (not shown) with the observations of Untersteiner (1960) (see Semtner 1976) over perennial sea ice shows the model to reproduce the seasonal evolution of surface temperature fairly faithfully, though, compared to the data, values are a little too high in spring and early winter.

Overall, the model underestimates the total sea ice extent for the Arctic and overestimates the amplitude of the seasonal variation of this quantity. Though the peak wintertime extents almost match the observed (figure 6), the spring meltback is too rapid with the result that for much of the year extents (and concentrations,

PHILOSOPHICAL TRANSACTIONS OF THE ROYAL SOCIETY A MATHEMATICAL, PHYSICAL & ENGINEERING SCIENCES

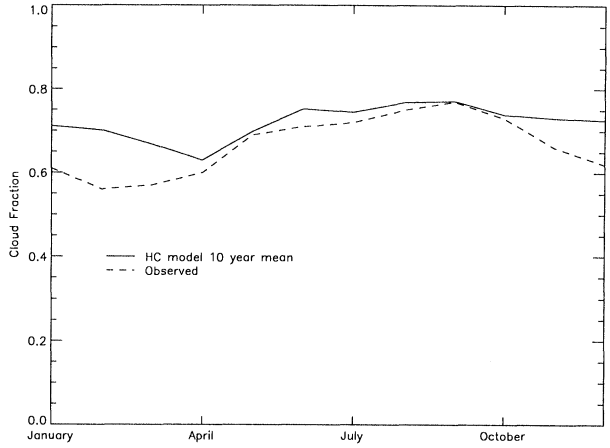

Figure 3. Seasonal variation of mean cloudiness polewards of 60° N as modelled (—) and derived from surface-based observations (- - -).

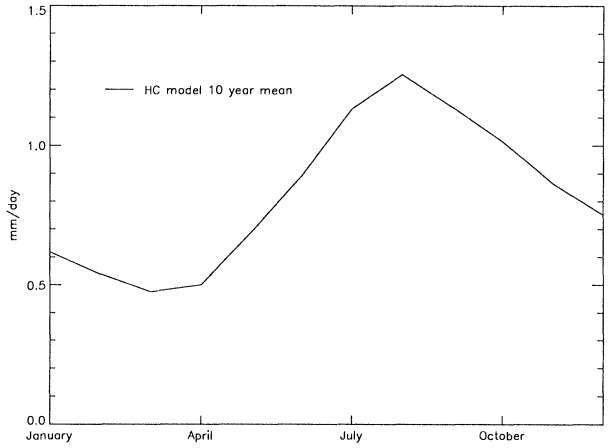

Figure 4. Seasonal variation of modelled total precipitation over the Arctic north of 75° N (mm day^{-1}).

particularly in summer) are markedly low. Ice thicknesses also tend to be too low in both winter and summer, with the model failing to achieve the thick ice (of order 5 m) observed to occur against the north coast of Greenland and the Canadian Archipelago. The model shows maximum ice thicknesses in the central Arctic of just over 3 m in March and some 2 m in September.

Over much of the Arctic basin, the seasonal cycle of freezing and melting of sea ice, coupled with inflow from the Arctic river systems combine to produce a surface layer of cold and relatively fresh water some tens of metres deep (figure 7*a*). Beneath this, to a depth of 100–150 m, lies the Arctic halocline in which salinity increases markedly with depth, but temperatures remain close to the freezing point. Below the halocline, salinity increases more slowly with depth, but temperatures increase quickly as the underlying layer of water of Atlantic origin is reached. Low resolution ocean models of the type used here employ large coefficients of viscosity for numerical stability reasons (Bryan *et al.* 1975) with the result that current strengths tend to be poorly simulated (higher resolution is precluded by available computing resources for

PHILOSOPHICAL TRANSACTIONS OF THE ROYAL SOCIETY A MATHEMATICAL, PHYSICAL & ENGINEERING SCIENCES

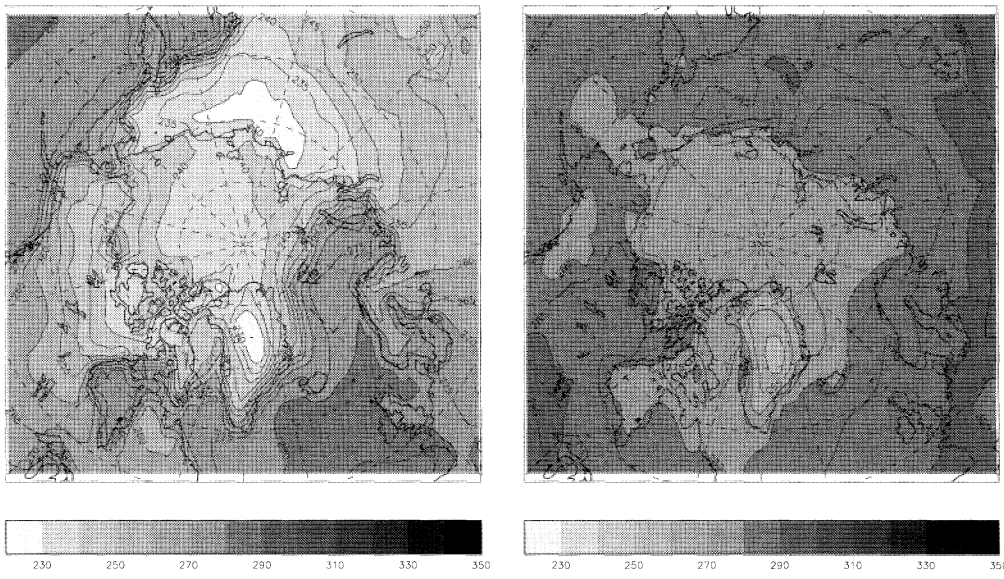

(a) (b)

Figure 5. Modelled surface temperature for (a) January and (b) July.

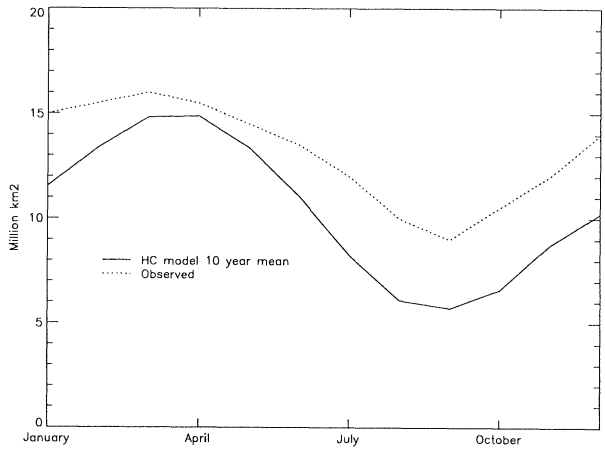

Figure 6. Seasonal variation of modelled (solid line) and observed (dotted line) total northern hemisphere ice extent. Observed values are digitized from Parkinson *et al.* (1987)

century-timescale runs). Nevertheless, the model clearly shows the inflow of Atlantic water into the Arctic basin (centred in this case at about 500 m). It also simulates (figure 7*b*) the effects of freshwater stabilization of the upper waters of the Arctic, but with a halocline which lacks the sharpness of the observed halocline and without reaching the correct degree of warmth in the nose of the temperature profile.

4. Simulation of Arctic climate change

Figure 8 shows predicted surface temperature change from an integration of the coupled model in which atmospheric concentrations of greenhouse gases (based on carbon dioxide, CO_2, as a surrogate) are increased at their observed rate from 1860

PHILOSOPHICAL TRANSACTIONS OF THE ROYAL SOCIETY A MATHEMATICAL, PHYSICAL & ENGINEERING SCIENCES

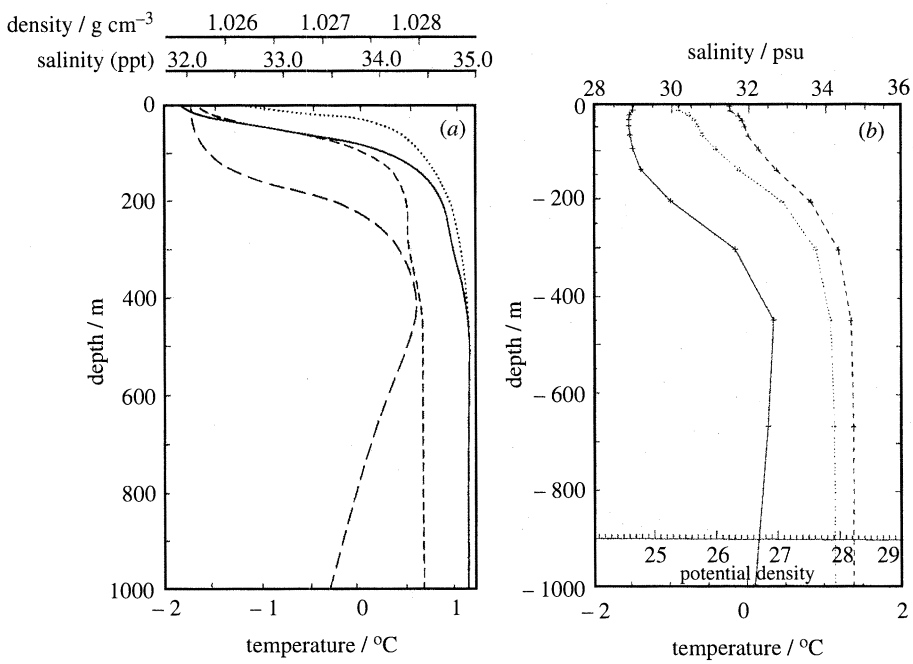

Figure 7. (*a*) Composite vertical distributions of temperature from Aagaard & Coachman (1975) (– –), salinity (—) and density (- - -) for the Arctic Ocean and salinity for the southern Eurasian basin (· · ·). (*b*) Model profiles for the Eurasian Arctic: —, temperature; - - -, salinity; · · ·, potential density.

to the present day and then increased further at 1% per annum (compound) into the future. For further details of the runs, see Hadley Centre (1995). The changes shown are for the decade 2020–2030, that of doubling of CO_2 concentrations in the model. Consistent with results from other models, the largest global temperature increases occur over the Arctic in winter (taken as the period December–February). Maximum temperature rises are associated with the marginal ice zone in the Atlantic sector and the regions of the shelf seas (figure 8*a*). Changes over the ice mass of Greenland lie between 2–4 °C. Introduction of a simple parametrization of the effects of sulphate aerosols reduces the magnitude of the warming, but changes the overall pattern very little (J. F. B. Mitchell, personal communication).

In summer (figure 8*b*), the temperature change over the Arctic is shown by the model to be small, since, as already noted, surface temperatures are constrained to the melting point of sea ice. Figure 9 shows the sea ice itself is reduced in thickness, by over 1 m in both summer and winter, with maximum changes coincident with the thickest ice in the control run.

Precipitation changes are shown in figure 10. The model predicts winter precipitation to be increased slightly over the central Arctic basin with higher local increases over the surrounding land masses. A general drying is shown over the region of the Greenland–Iceland–Norwegian (GIN) Sea, but with increases over the Atlantic-sector marginal ice zone. In summer, there is a tendency towards reduced precipitation around the periphery of the Arctic Ocean, with regions of both slight increase and decrease in the central basin. The precipitation changes show some sensitivity to introduction of aerosol effects in the model formulation. These result in an increase

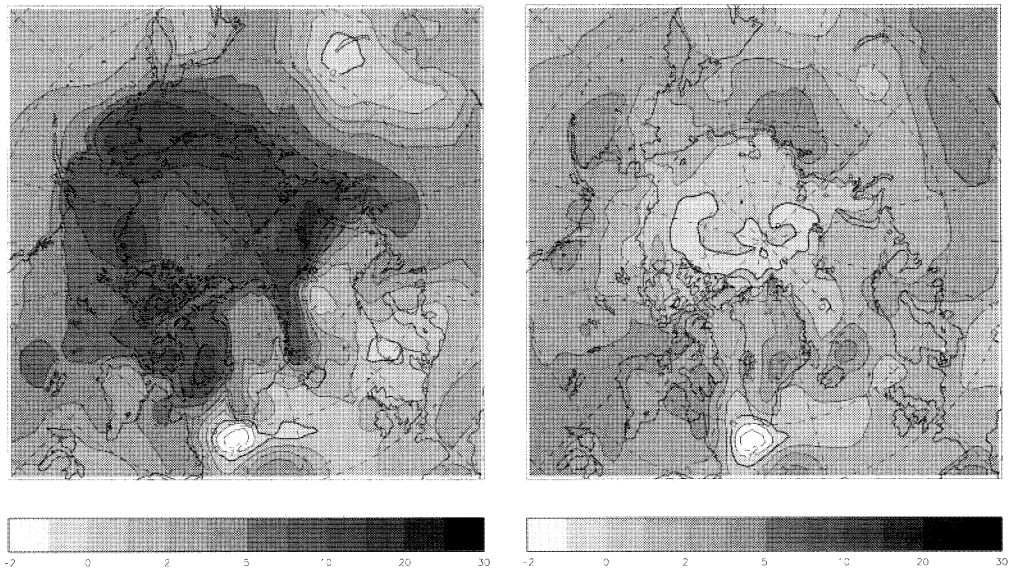

Figure 8. Temperature change over the Arctic for the decade of doubling of carbon dioxide from a run of the Hadley Centre model with transiently increasing greenhouse gases: (*a*) winter (December–February) and (*b*) summer (June–August).

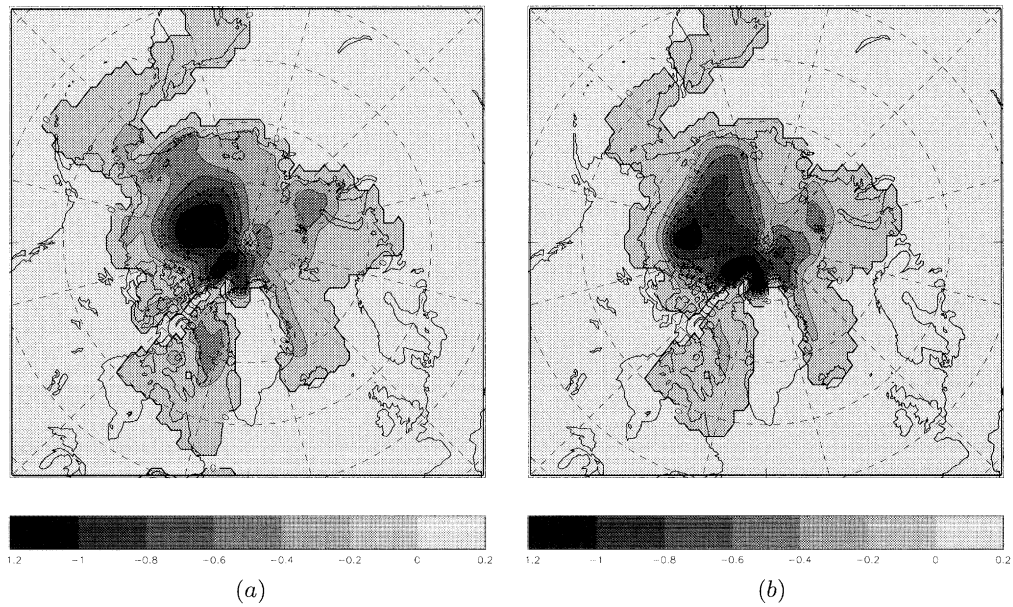

Figure 9. As figure 8, but for change in sea ice thickness.

in the areas of reduced precipitation in over the land areas around the periphery of the Arctic in winter, and more generally in summer.

PHILOSOPHICAL TRANSACTIONS OF THE ROYAL SOCIETY A MATHEMATICAL, PHYSICAL & ENGINEERING SCIENCES

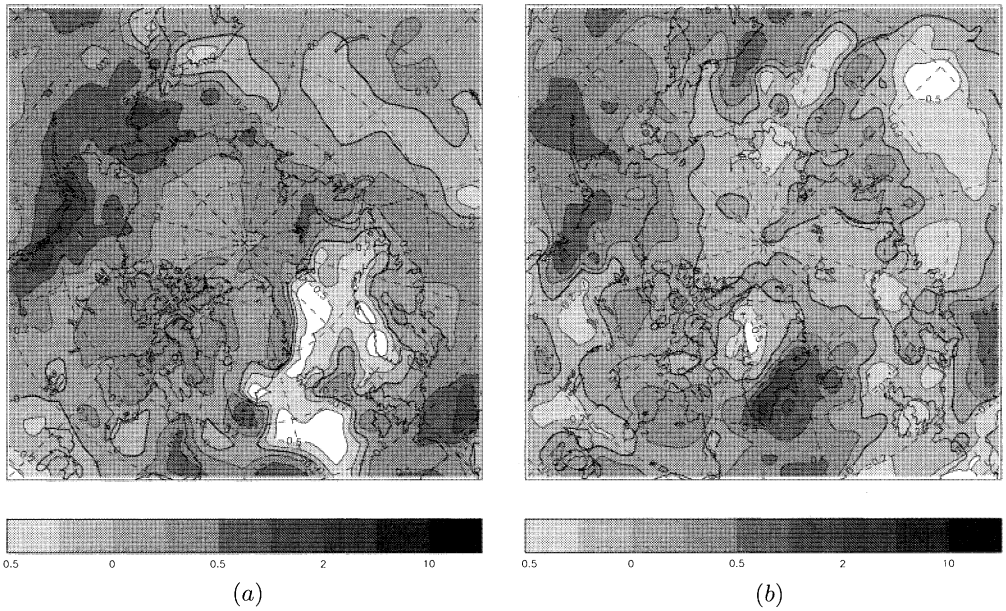

(*a*) (*b*)

Figure 10. As figure 8, but for change in precipitation.

5. Concluding remarks

Consistent with other model simulations, the Hadley Centre model shows the Arctic to be a region of high sensitivity to increased greenhouse gas concentrations in winter. The largest temperature changes over the Arctic Ocean are to be found in the region of the marginal ice zone and the shelf seas, and there is a generally reduced ice thickness over the central Arctic, with largest values (of over 1 m) coincident with the thickest ice in the control simulation. There is a general small increase in precipitation over the Arctic in winter and regionally variable small increases and decreases in summer.

It must, of course, be born in mind that, as already noted, confidence in predictions on a regional basis using global coupled models is still, as yet, relatively low. Comparison of results of Arctic warming in previous transient response experiments by different centres certainly reveals large differences between models (Rowntree 1993). Uncertainties in both an Arctic and wider, global context are associated, in particular, with sulphate aerosols, clouds, ocean resolution, representation of sea ice processes and representation of runoff into the Arctic. Nevertheless, the comparison of model and observed climatology shown here is encouraging and helps to give credence to the large-scale characteristics of the predictions.

Many people within the Hadley Centre have been involved in the development of the coupled model described here and their contribution is gratefully acknowledged. Particular thanks are due to Dr T. C. Johns and Dr S. F. B. Tett and who ran the experiments described in this paper.

References

Aagaard, K. & Coachman, L. K. 1975 Toward an ice-free Arctic Ocean. *EOS* **56**, 484–486.

Bryan, K., Manabe, S. & Pacanowski, R. C. 1975 A global ocean–atmosphere climate model. II. The oceanic circulation. *J. phys. Oceanogr.*, **5**, 30–46.

PHILOSOPHICAL TRANSACTIONS OF THE ROYAL SOCIETY A MATHEMATICAL, PHYSICAL & ENGINEERING SCIENCES

Cox, M. D. 1984 A primitive equation, 3-dimensional model of the ocean. *GFDL Ocean Group tech. Rep.* No. 1. Princeton, NJ: Geophysical Fluid Dynamics Laboratory.

Cubasch, U., Hasselmann, K., Hock, H., Maier-Reimer, E., Mikolajewicz, U., Santer, B. D. & Sausen, R. 1992 Time dependent greenhouse warming computations with a coupled ocean–atmosphere model. *Climate Dyn.* **8**, 55–69.

Cullen, M. P. J. 1993 The unified forecast/climate model. *Meteorol. Mag.* **122**, 81–94.

Gregory, D. & Rowntree, P. R. 1990 A mass flux convection scheme with representation of cloud ensemble characteristics and stability dependent closure. *Mon. Weather Rev.* **118**, 1483–1506.

Hadley Centre 1995 *Modelling Climate Change 1860–2050.* Bracknell: Hadley Centre, Meteorological Office.

Hibler, W. D. III 1979 A dynamic-thermodynamic sea ice model. *J. phys. Oceanogr.* **9**, 817–846.

Houghton, J. T., Jenkins, G. J. & Ephraums, J. J. (eds) 1990 *Climate change: the IPCC scientific assessment.* Cambridge University Press.

Houghton, J. T. Callander, B. A. & Varney, S. K. (eds) 1992 *Climate change 1992: the supplementary report to the IPCC scientific assessment.* Cambridge University Press.

Ingram, W. J., 1990 Radiation. *Meteorological Office unified model documentation paper No. 23.* Bracknell: National Meteorological Library. (Unpublished.)

Kraus, E. B. & Turner, J. S. 1967 A one dimensional model of the seasonal thermocline. II. The general theory and its consequences. *Tellus* **19**, 98–106.

Legates, D. R. & Willmott, C. J. 1990 Mean seasonal and spatial variability in gauge-corrected global precipitation. *Int. J. Climatol.* **10**, 111–127.

Manabe, S., Stouffer, R. J., Spelman, M. J. & Bryan, K. 1991 Transient responses of a coupled ocean–atmosphere model to gradual changes of atmospheric CO_2. Part 1. Annual mean response. *J. Climate* **4**, 785–818.

Manabe, S., Spelman, M. J. & Stouffer, R. J. 1992 Transient responses of a coupled ocean–atmosphere model to gradual changes of atmospheric CO_2. Part 2. Seasonal response. *J. Climate* **5**, 105– 126.

Manabe, S. & Stoufer, R. J. 1980 Sensitivity of a global climate model to an increase in CO_2 concentration in the atmosphere. *J. geophys. Res.* **85**, 5529–5554.

Mitchell, J. F. B. & Murphy, J. M. 1995 Transient response of the Hadley Centre coupled ocean–atmosphere model to increasing carbon dioxide. Part 2. Spatial and temporal structure and response. *J. Climate* **8**, 57–80.

Murphy, J. M. 1995 Transient response of the Hadley Centre coupled ocean–atmosphere model to increasing carbon dioxide. Part 1. Control climate and flux adjustment. *J. Climate* **8**, 36–56.

Orwig, S. (ed.) 1970 *World survey of climatology*, vol. 14. *Climates of the polar regions.* Amsterdam: Elsevier.

Pacanowski, R. C. & Philander, S. G. H. 1981 Parametrization of vertical mixing in numerical models of tropical oceans. *J. phys. Oceanogr.* **11**, 1143–1451.

Palmer, T. N., Schutts, G. J. & Swinbank, R. 1986 Alleviation of systematic bias in general circulation and numerical weather prediction models through orographic gravity wave drag parametrization. *Q. Jl R. Met. Soc. Lond.* **112**, 1001–1039.

Parkinson, C. L., Comiso, J. C., Cavalieri, D. J., Gloersen, P. & Campbell, W. J. 1987 *Arctic sea ice, 1973–1976,* NASA SP-489.

Redi, M. H. 1982 Oceanic isopycnal mixing by coordinate rotation. *J. phys. Oceanogr.* **12**, 1154–1158.

Rowntree, P. R. 1993 Global and regional patterns of climate change: recent predictions for the Arctic. *Clim. Res. tech. Note* No. 43. Bracknell: Meteorological Office.

Semtner, A. J. Jr. 1986 A model for the thermodynamic growth of sea ice in numerical investigations of climate. *J. Phys Oceanogr.* **6**, 379–389.

Smith, R. N. B. 1990 A scheme for predicting layer clouds and their water content in a general circulation model. *Q. Jl R. Met. Soc. Lond.* **116**, 435–460.

PHILOSOPHICAL TRANSACTIONS OF THE ROYAL SOCIETY A MATHEMATICAL, PHYSICAL & ENGINEERING SCIENCES

Taylor, N. K. & Bunton, C. 1993 River runoff in the new UKMO coupled model. *Research Activities in Atmospheric and Oceanic Modelling* (ed. G. J. Boer), Report No. 18, WMO/TD-No. 553. Geneva: World Meteorological Organisation.

Warrilow, D. A., Sangster, A. B. & Slingo, A. 1986 Modelling of land surface processes and their influence on European climate. *Dyn. Clim. tech. Note* No. 38. Bracknell: Meteorological Office.

Washington, W. M. & Meehl, G. A. 1986 General circulation model CO_2 sensitivity experiments: sea ice albedo parametrizations and globally averaged surface air temperature. *Clim. Change* **8**, 231–241.

Wilson, C. A. & Mitchell, J. F. B. 1987 A doubled CO_2 sensitivity experiment with a GCM including a simple ocean. *J. geophys. Res.* **92**, 13315–13343.

Discussion

D. J. Drewry (*NERC, Swindon, UK*). Model validation and interpretation of model results rely fundamentally upon accurate observations. In the Arctic there are only very limited and spatially patchy datasets: time series of data are short in duration. How do these limitations influence and affect the Arctic and regional predictions?

H. Cattle. The models do simulate the gross features of Arctic climate. However, while the models represent the important feedbacks in the climate system, their details are imperfectly represented and this will affect the predictions in a way which is difficult to quantify. An increased observational database for the Arctic is certainly needed both for model verification and for better representation in models of Arctic physical processes. This is a primary aim of, for example, the World Climate Research Programme 10-year Arctic Climate System Study.

PHILOSOPHICAL TRANSACTIONS OF THE ROYAL SOCIETY A MATHEMATICAL, PHYSICAL & ENGINEERING SCIENCES

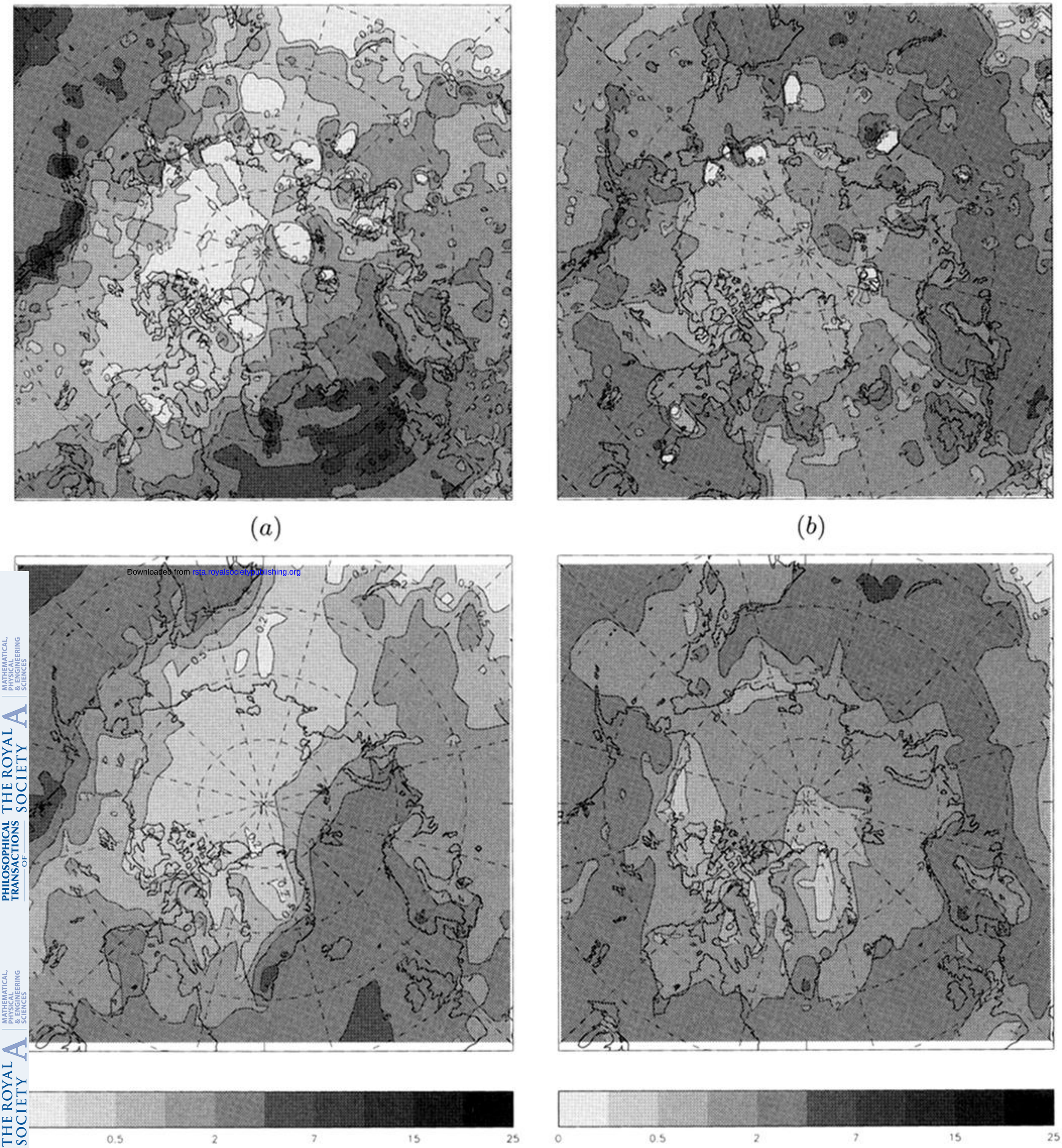

Figure 2. As figure 1, but for precipitation. Observed fields are derived from the dataset of Legates & Willmott (1990).

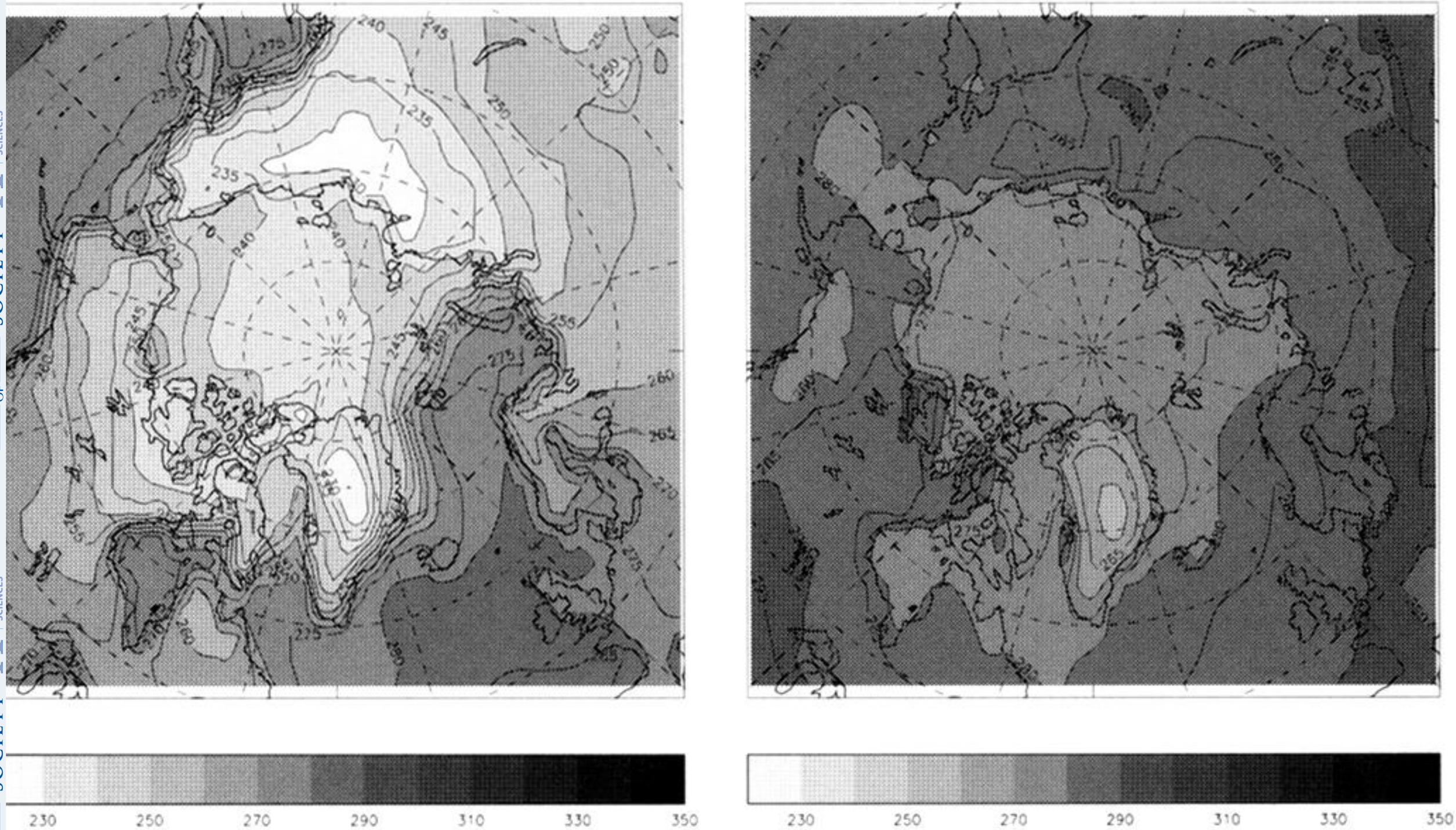

Figure 5. Modelled surface temperature for (*a*) January and (*b*) July.

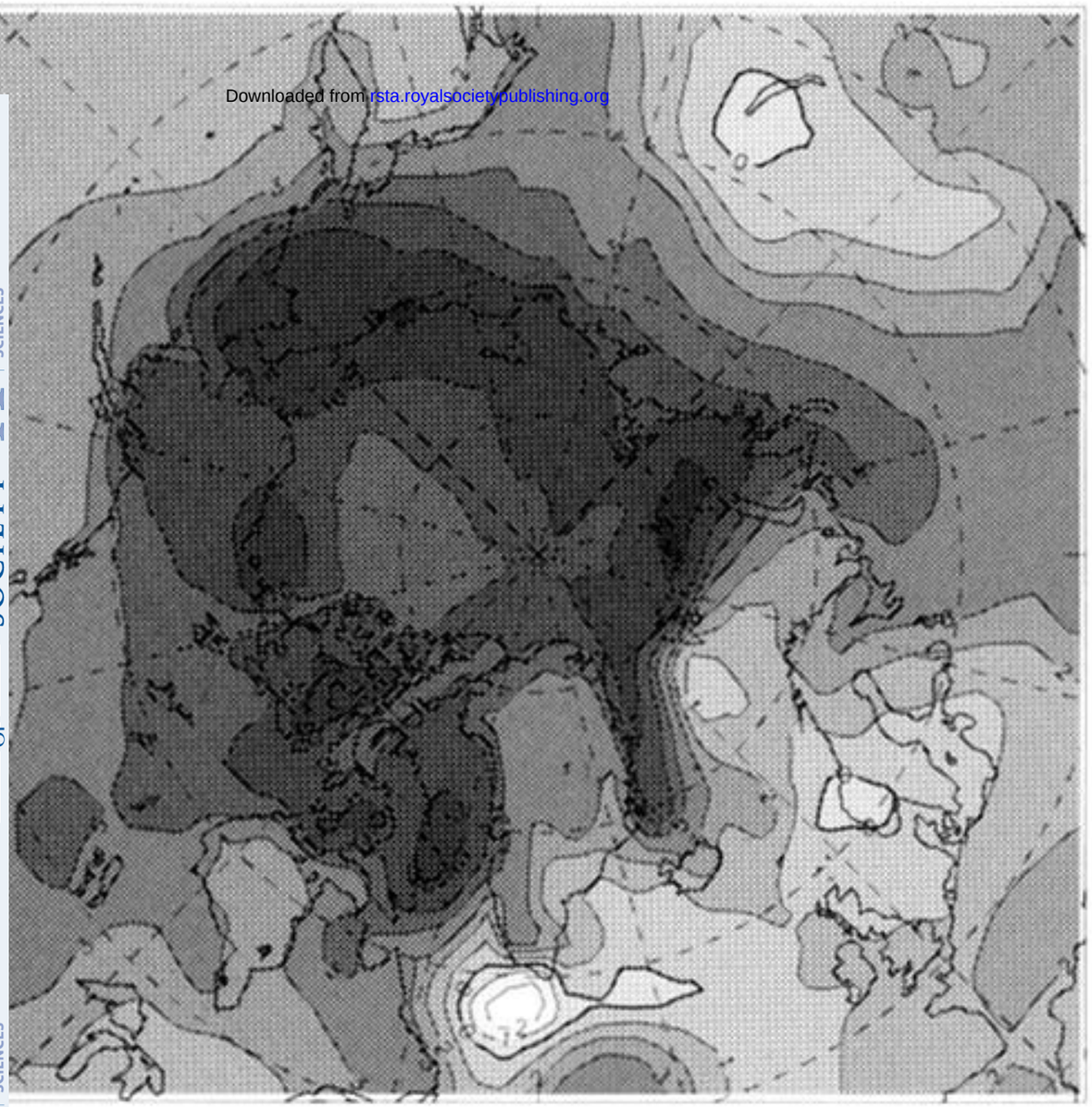

(a)

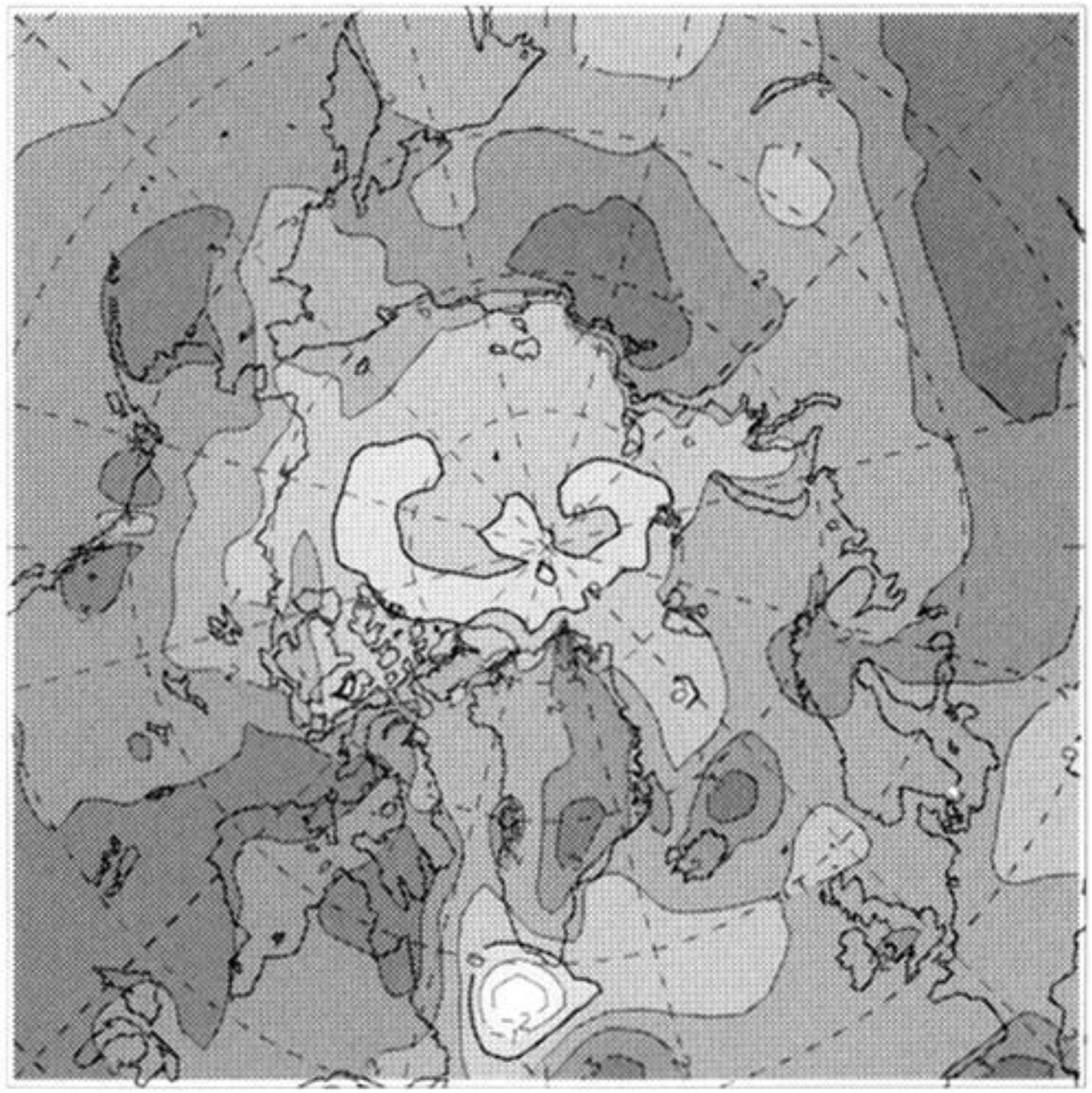

(b)

igure 8. Temperature change over the Arctic for the decade of doubling of carbon dioxide om a run of the Hadley Centre model with transiently increasing greenhouse gases: (*a*) winter December–February) and (*b*) summer (June–August).

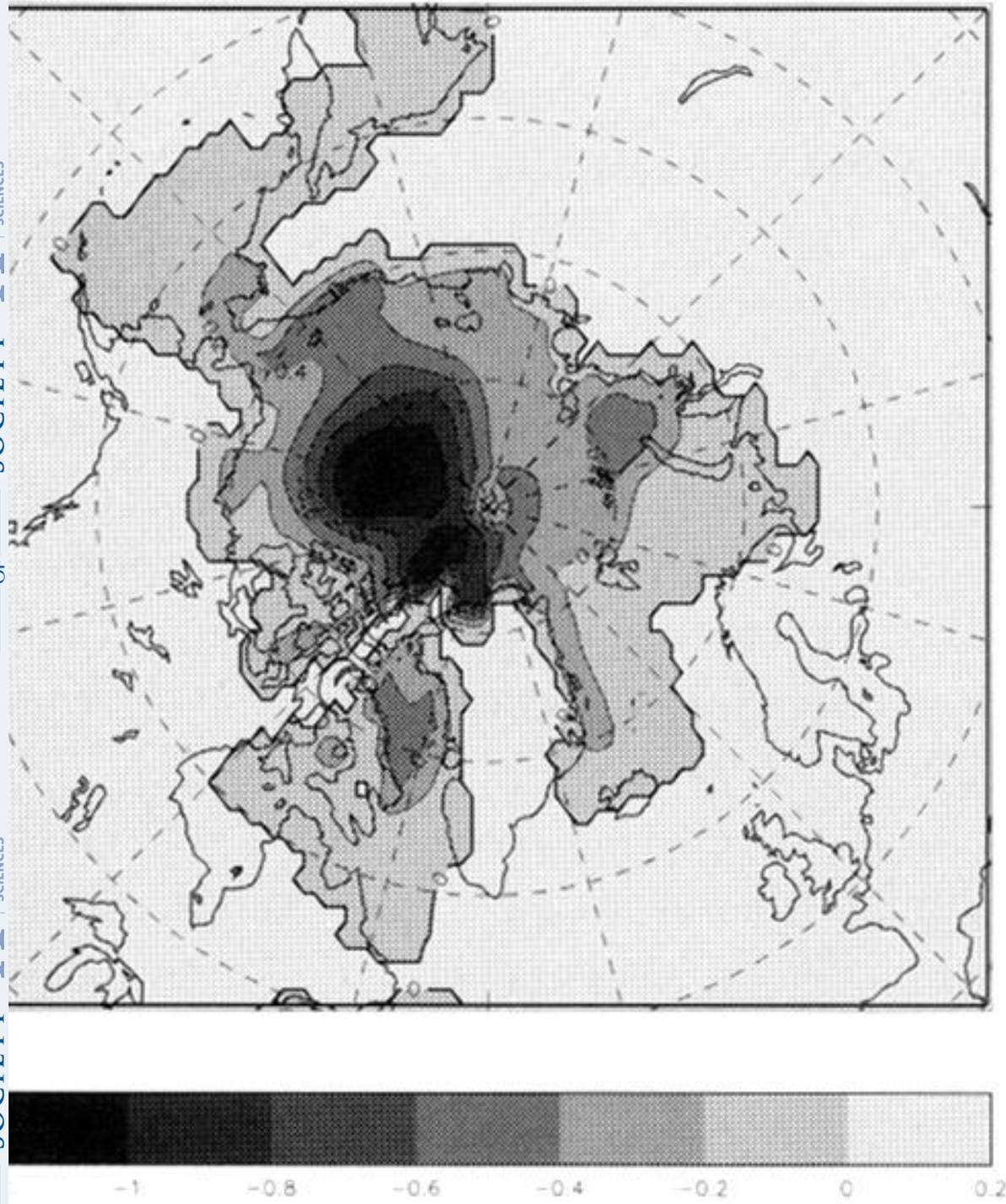

(a)

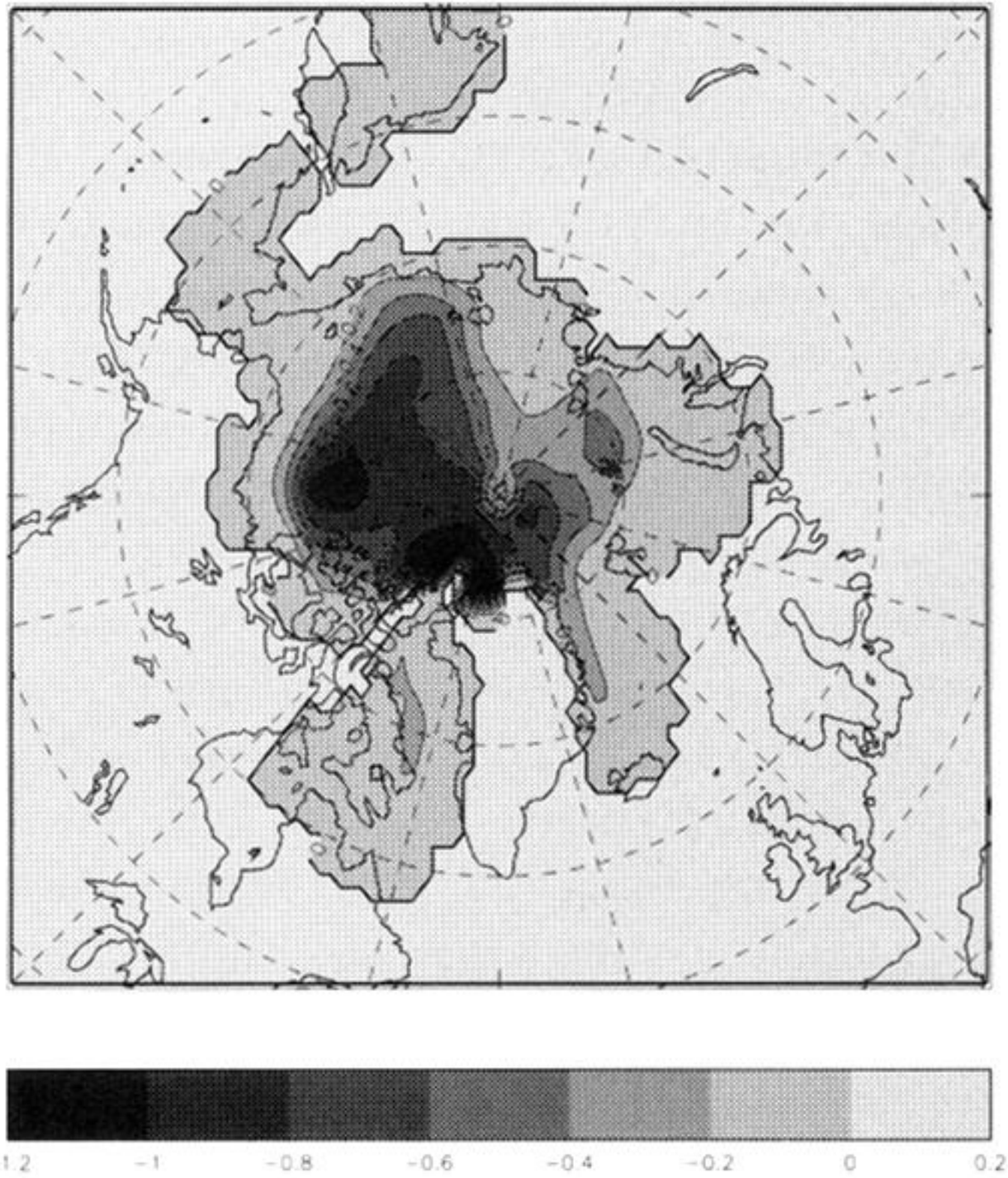

(b)

Figure 9. As figure 8, but for change in sea ice thickness.

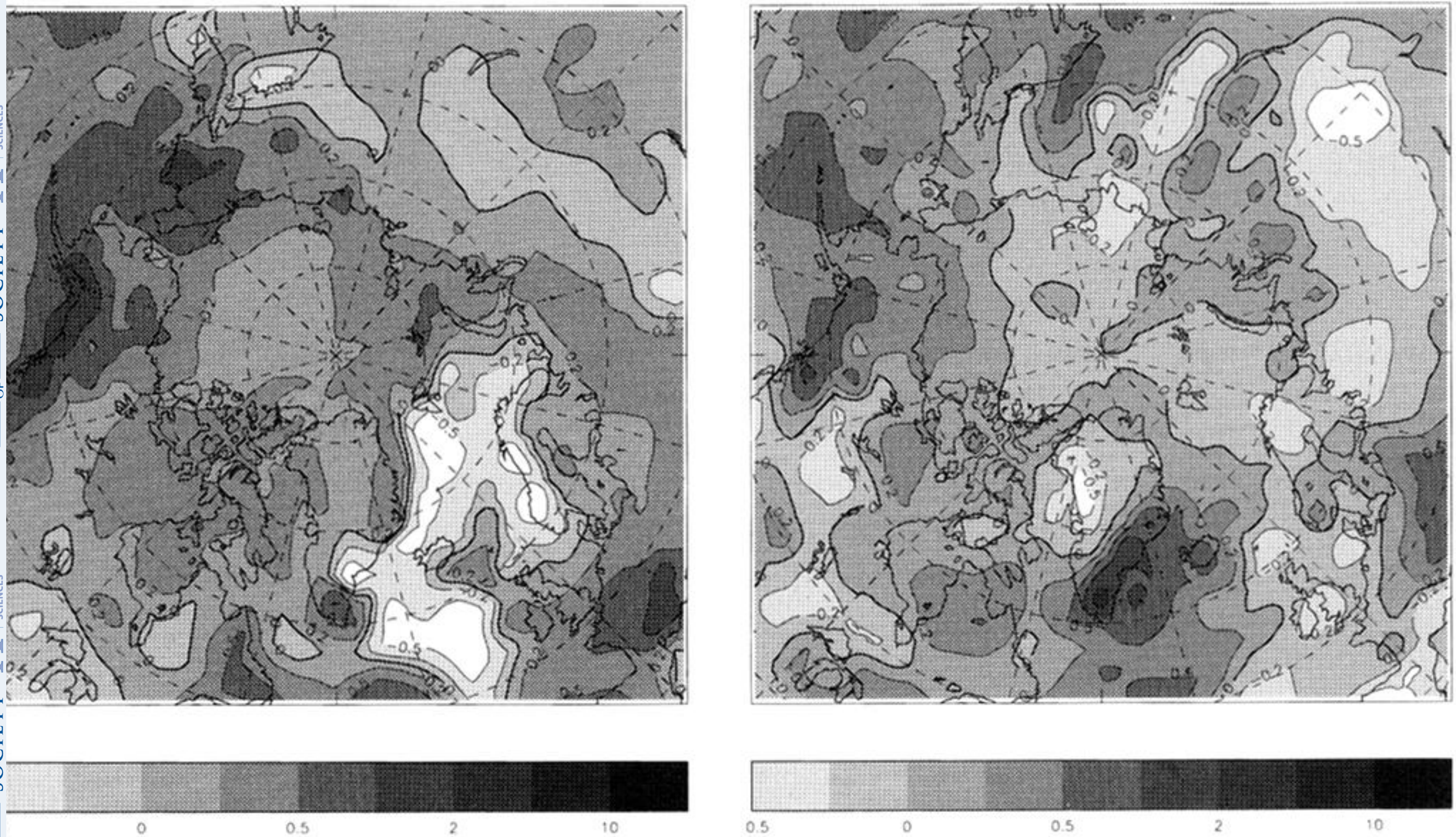

Figure 10. As figure 8, but for change in precipitation.